International Journal of Chemical Studies

P-ISSN: 2349–8528
E-ISSN: 2321–4902
www.chemijournal.com
IJCS 2022; 10(6): 20-24

Received: 12-09-2022
Accepted: 17-10-2022

Dr. Jaidev Kumar
Assistant Professor in Hariom Saraswati (PG) College, Dhanauri, Haridwar, Uttarakhand, India

Corresponding Author:
Dr. Jaidev Kumar
Assistant Professor in Hariom Saraswati (PG) College, Dhanauri, Haridwar, Uttarakhand, India

Photoluminescence excitation spectra of ZnS nanoparticles at different temperature

Dr. Jaidev Kumar

Abstract
Nanotechnology is a promising field of interdisciplinary research. The potential uses and benefits of nanotechnology are enormous. Nanotechnology is the technology of 21st century i.e. Nanotechnology is the science of the extremely small particles holds enormous potential applications for environment. Nanotechnology is the science of materials at the molecular or subatomic level. It involves engineering of particles smaller than 100 nanometers (one nanometer is one-billionth of a meter) and the technology involves developing materials or devices within that size is invisible to the human eye and often many hundred times thinner than the width of human hair. The physics and chemistry of materials are radically different when reduced to the nanoscale; they have different strengths, conductivity and reactivity, physical, chemical, biological, thermal, electrical properties. Nanotechnology has been described as the development of clean technologies, to minimize potential environmental and human health risks associated with the manufacture and use of nanotechnology products and to encourage replacement of existing products with new nano-products that are more environmentally friendly throughout their lifecycle. Most applications of Nanoparticles in reducing natural disasters can be analyzed in three main areas that are building materials, sensors and medicine.

Keywords: Nanotechnology, environment nanotechnology, nanoproducts, nanosensors, nanomedicine

Introduction
Nanotechnology and science of nanomaterials provide apt potential in engineering of materials and at present is the enormously growing and developing scientific technology. It is defined as the study of controlling, manipulating and creating systems based on their atomic or molecular specifications [1]. As stated by the US National Science and Technology Council, the essence of nanotechnology is the ability to manipulate matters at atomic, molecular and supra-molecular levels for creation of newer structures and devices [2]. Generally Nanotechnology deals with structures sized between 1 to 100 nanometre (nm) in at least one dimension and involves in modulation and fabrication of nanomaterials and nanodevices. It has been endured as an area of intense scientific research in various fields like optical, electronic and biomedical fields. Bacterial cells, plant cells and mammalian cells which are more than 100 nm size can easily engulf or internalize the particulates of nano-size like viruses (75-100 nm), proteins (5-50 nm), nucleic acids (2 nm width) and atoms (0.1 nm). If we compare a single human hair diameter (50 µm) to 1 nm nanofibers, hair will be 50,000 times larger than the size of 1 nm [3]. The great visionary late Nobel Physicist Richard P Feynman first designed the idea of molecular manufacturing in 1959. The legendary scientist who first suggested that devices and materials could someday have atomic specifications and that this development path cannot be avoided [4].
For years this science have engaged scientist in exploring the very unique physico-chemical properties of nanoparticles. In field of Nanotechnology due to increase in surface to volume ratio and quantum confinement, the physical, chemical, thermal, electrical, optical and biological properties of a nanomaterial are drastically changes [5].

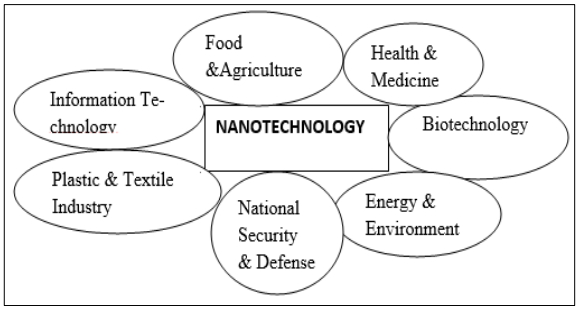

Methodology

Nanotechnology is an interdisciplinary research field, several methods are used in fabrication of nanomaterials such as Physical (mechanical and vapor deposition techniques), Chemical (Colloids, Sol-gel, L-B films etc.), Biological (Bio membranes, DNA etc) and Hybrid (Electrochemical, CVD etc). The guiding principle for the technique, to be employed for synthesis, depends largely upon, (a) material of interest, (b) type of nanostructure (0D, 1D, 2D, 3D), and (c) size and quantity etc. There are two basic approaches for manufacturing nanomaterials, (i) Top down approach (ii) Bottom up approach. In top-down approach, we reduce the size of material upto nano size, where as in bottom up approach, we start from atomic size and collecting atoms to nano size.

Among various methods for fabrication of nanomaterials the 'wet chemical method is the simplest one because of following considerations

A. Inexpensive, least instrumentation required as compared to Physical Methods,
B. Moderate temperature (< 350 °C) is required for most of nanomaterials,
C. Dopant can be easily inserted during synthesis process,
D. Nanomaterials of different size and shapes are possible. Materials so obtained can be dried to obtain powder and thin films.

Preparation of ZnS Nanoparticles

Although various methods are available for the synthesis of ZnS nanoparticles, chemical precipitation is widely being used for the preparation of colloidal nanoparticles as the possibility of cluster formation is very less in this method when compared to the other methods. Here, 0.27 g of $ZnCl_2$ (1/10 M, 20 ml) solution and 0.1M Na_2S solution were prepared in distilled water and were first refluxed for an hour separately. 50 ml Na_2S solution was then added to the mercaptoethanol solution of 0.25 ml (10^{-2} M) and then 20 ml $ZnCl_2$, which was continuously refluxed to get a colloidal form of ZnS. The colloidal sample was refluxed for another 20 min at 80 °C for uniform distribution of the particles. Then this was filtered out and washed with distilled water and ethanol for removing the additional impurities formed during the preparation process. The filtrate was dried at room temperature, which yields high-quality ZnS nanocrystals.

The X-ray diffraction of the sample at room temperature is taken by a powder X-ray diffratometer (Rigaku Miniflex-II). The transmission electron micrograph of the sample is taken by a transmission electron microscope (Jeol JEM-100cx). The absorption and luminescence spectra for ZnS nanoparticles were recorded using UV-Visible spectrophotometer (Shimadzu UV-2450) and spectrofluorometer (Shimadzu RF-5310) respectively.

The dielectric measurement of the sample of thickness 2.06 mm and diameter 10.41 mm was carried out using gold electrodes by an LCR meter (Hioki) in the frequency range from 100 Hz to 1 MHz and in the temperature range from 298 K to 373 K. The temperature was controlled with a programmable oven. All the dielectric data were collected while heating at a rate of 1^0C min^{-1}. The complex electric modulus M^* ($=1/\varepsilon^*$) and impedance Z^* ($=M^*/j\omega C_o$) are obtained from the temperature dependence of the real (ε') and imaginary (ε'') components of the dielectric permittivity ε^* ($=\varepsilon'-j\varepsilon''$) and $\varepsilon''=\varepsilon' \tan\delta$.

Results and Discussion

Fig. 2 shows the X-ray diffraction pattern of the sample taken at room temperature. The broadening of the diffraction peaks is primarily due to the finite size of the Nano crystallites and is quantitatively analyzed by the Debye-Scherer formula

$$L = \frac{0.94\lambda}{B\cos\theta} \quad (1)$$

Where

L is the average size of the particle, λ is the wavelength of X-ray radiation, B is the full width at half maximum (FWHM) and θ is the diffraction angle. According to the data in Fig. 1 and given formula, the average particle size of the material is found to be 45 nm. The transmission electron micrograph of the ZnS is shown in the inset of Fig. 1. The average grain size of the Nano clusters of ZnS is found to be 50 nm. Particle size analyzed by XRD and TEM are in good agreement.

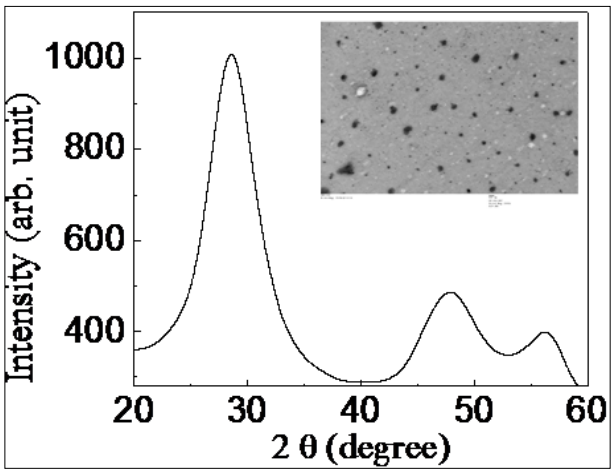

Fig 2: The XRD (TEM micrograph shown in the inset) for ZnS.

The inset of Fig. 3 shows the UV-visible spectra of ZnS nanoparticles in the absorbance range of 200-350 nm. The absorbance peak at 277 nm is blue shifted compared to the bulk ZnS for which absorption peak is at 345 nm. The blue-shifted absorption edge is due to the quantum confinement of the exactions present in the sample, resulting in a more discrete energy spectrum of the individual nanoparticles. The broadening of the absorption spectrum is mainly due to the quantum confinement of the ZnS nanoparticles. The effect of the quantum confinement on impurity critically depends on the size of the host crystal. As the host decreases, the degree of confinement and its effect increases. The band gap energy is increased (~4.1 eV) compared to that (~3.6 eV) of bulk ZnS shown in the Fig. 2, the enlargement of the band gap can be attributed to the quantum confinement effect of the ZnS nanoparticles.

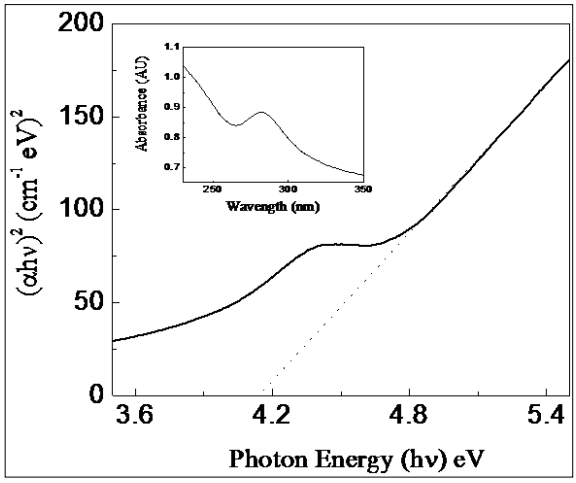

Fig 3: Energy band gap determination of ZnS nanoparticles. The UV-visible absorption spectra of the ZnS nanoparticles shown in the inset.

Fig. 4 shows the PL emission (a) and excitation (b) spectra of ZnS nanoparticles. It shows strong blue-luminescence with peak maximum around 335 nm and a side band at 352 nm. The corresponding excitation spectra with peak maximum at 420 nm indicate energy-transfer from the band-to-band electronic excitation of the quantum confined ZnS [11].

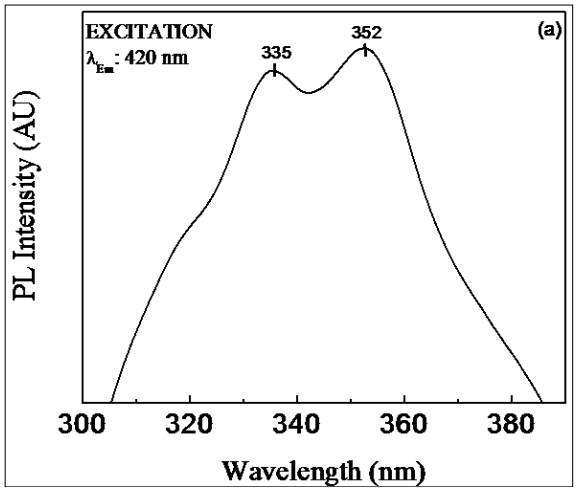

Fig4: Photoluminescence emission spectra of ZnS nanoparticles.

With the self-aggregation of nanoparticles, the excitation spectra also show reduction in the intensity but more significantly, a gradual red-shift in the peak maximum with larger line broadening. The origin of the blue-luminescence of ZnS nanoparticles has been studied by different groups [11, 12]. Highly asymmetric and broadened emission band with multiple peak maxima indicate the involvement of different luminescence centers in the radioactive process. The nanoparticles prepared under sulphur deficient synthetic condition of S^{2-}/Zn^{2+} will have larger concentration of sulphur vacancies (VS).

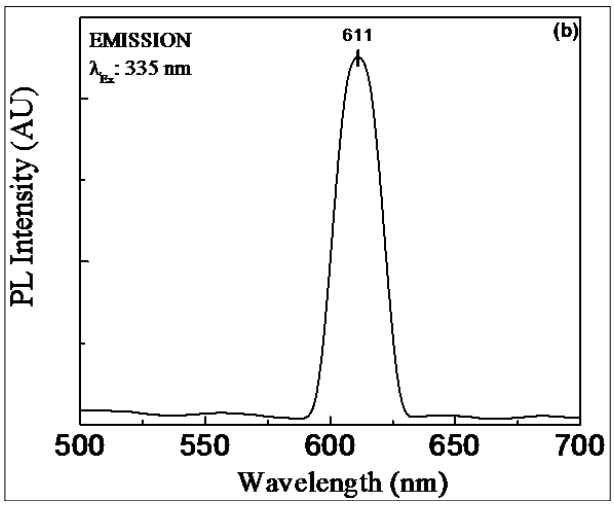

Fig 5: Photoluminescence excitation spectra of ZnS nanoparticles.

It is reported that sulphur vacancies can act as doubly ionized electron trap centers and facilitate VS/VB (valence band) and/or VS/SS (surface states, including interstitial defects and impurities) [11]. Though the lattice vacancies are point defects, due to the large surface-to-volume ratio of nanoparticles, the concentration of these defects will be more at the surface regions than the interiors. Therefore, in the ZnS nanoparticles with unmodified surfaces, the effect of surface states will be dominant as seen by the strong blue luminescence. However, the observed quenching of these emission bands with the self-assembly of nanoparticles suggests that the vacancy centers are annihilated during the particle-to-particle attachment/interface precipitation by way of incorporation of more and more crystal growth units at the nanoparticles surfaces.

Fig. 6 shows a complex-plane impedance plot (Z^*) of ZnS, plotting the imaginary part Z'' against the real part Z'. In general, for a perfect crystal, the values of resistance R and capacitance C can be analyzed by an equivalent circuit of one parallel resistance-capacitance (RC) element. This RC element give rise to one semicircular arc on the complex plane and has intercepts on the Z' axis of zero and R. Thus, C can be calculated with the relation $\omega_m RC=1$, where $\omega_m=2\pi\nu_m$ and ν_m is the frequency at the arc maxima.

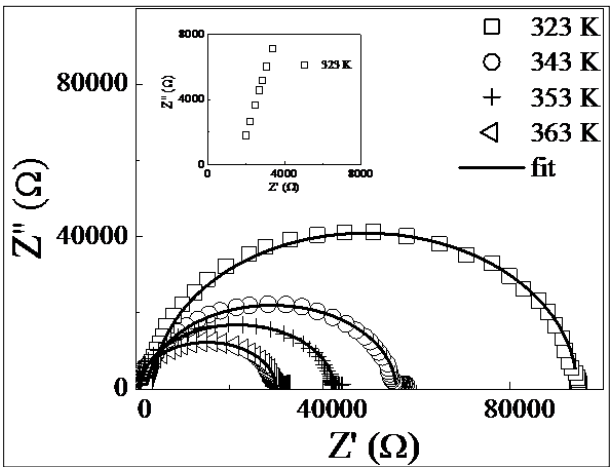

Fig 6: The complex-plane impedance plot with the corresponding equivalent circuit is shown for ZnS at various temperatures. The solid line is the best fit for ZnS. The inset shows expanded views of the high-frequency data near the origin at 323 K.

For a nano crystal containing interfacial boundary layers, the equivalent circuit may be considered as two parallel RC elements connected in serial and giving rise to two arcs in complex plane: one for the nano crystal (grain) and the other for the interfacial boundary (grain-boundary) response. The relative position of the two arcs in the complex plane can be identified by the frequency. Based on the equivalent circuit consisting of two parallel RC elements in series, the nonzero intercept on the Z'-axis (at 323 K) indicates the presence of an arc with ω_{max} higher than the maximum frequency measured (1 MHz).

Dielectric relaxation observed in electro ceramics are better analysed using the simplified equivalent circuits consisting of two parallel RC circuits connected in series, one RC element, R_g C_g, representing the grain, and the other $R_{gb}C_{gb}$, representing the grain boundary [13, 14], as shown in the inset of Fig. 4. Here, R_g, C_g and R_{gb}, C_{gb} are the resistance and capacitance associated with the grain and the grain boundary, respectively. Each parallel RC element results in a semicircle in the impedance plots. Fig. 6 shows a complex impedance Z* (Z" versus Z') plot for ZnS nanoceramics, obtained by plotting the imaginary part (Z") against the real part (Z') in the 323 K–363 K temperature range. The high frequency impedance response of the sample in the 323 K–363 K temperature range has been highlighted in Fig. 5 to show the evolution of the high frequency semicircle.

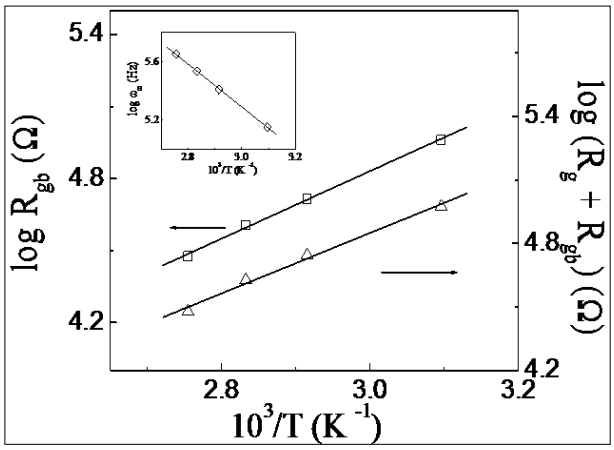

Fig 7: Arrhenius plot for the grain boundary resistance (Rgb) and total grain. The insetshows grain boundary relaxation frequency (ω_{gb}) for ZnS nanoceramics. The solid line is the best fit for the Arrhenius equations.

The equivalent electrical equation can be represented by

$$Z' = \frac{R_g}{1+(\omega R_g C_g)^2} + \frac{R_{gb}}{1+(\omega R_{gb} C_{gb})^2} \quad (2)$$

$$Z'' = R_g\left(\frac{\omega R_g C_g}{1+(\omega R_g C_g)^2}\right) + R_{gb}\left(\frac{\omega R_{gb} C_{gb}}{1+(\omega R_{gb} C_{gb})^2}\right) \quad (3)$$

The best fitting of RC equivalent circuit by solid line for 323 K, 343 K and 363 K with two semicircular arc of R_g and R_{gb} is shown in the table 1.

Conclusion

The resistance values of the grains and the grain boundaries are obtained from the intercepts of the corresponding semicircles with the real axis (Z') (diameter of each semicircle) which gives R_g and R_{gb}, respectively. The resistance obtained for the total resistance or dc resistance of the sample log (R_g + R_{gb}) and log R_{gb} is plotted in the Arrhenius format in the Fig. 6, obey the Arrhenius law with activation energy of 0.28 eV and 0.27 eV respectively. Plot of log (ω_{gb}) (relaxation frequency of grain boundary) (inset of Fig. 5) reveal that ω_{gb} follow an Arrhenius law associated with activation energies of 0.28 eV. Furthermore, as it is clear from Fig. 5, R_{gb} + R_g are only slightly higher than R_{gb} in the entire temperature range under study. Hence, it could be concluded that R_{gb} >> R_g, so that in the entire temperature range C_{gb} >> C_g.

References

1. Feynman R. There's plenty of room at the bottom. Science. 1991;254:1300-1301.
2. Tripathi R, Kumar A, Sinha TP, Pramana J Phys. June 2009;72(6):969-978.
3. Ramna Tripathi, Akhilesh Kumar, Chandrahas Bhati, Sinha TP, Current Appl. Phys. 2010;10:676-681.

4. Stirling 'Opportunities for Industry in the Application of Nanotechnology; Institute of Nanotechnology'; c2000.
5. Drexler KE. MIT, USA, Ph.D. Thesis entitled 'Nanosystems: Molecular Machinery, Manufacturing and Computation; c1991.
6. Drexler KE. Nanosystems Molecular Machinaery, Manufacturing and Computation, John Wiley. Robert A. Freitas Jr., Introduction to Nanomedicine; c2000.
7. National Cancer Institute, Cancer Nano technology: Going small for big advances, NIH publication, Jan 2004.
8. Brigger C, Bubernet. Couvreur P. Advanced Drug Delivery Reviews. 2002:54:631-651.
9. Roy I, Ohulchansky TY, Pudavar HE, Bergey EJ, Oseroff AR, Morgan J, Dougherty TJ, Prasad PN. J Am Chem Soc. 2003;125:7860-7865.
10. Reich DH, Tanase M, Hultgren A, Bauer LA, Chen CS, Meyer GJ. J Appl Phys. 2003;93:7275-7280.
11. Weissleder R, Elizondo G, Wittenburg J, Rabito CA, Bengele HH, Josephson L. Radiology. 1990;175:489-493.
12. O'Neal DP, Hirsch LR, Halas NJ, Payne JD, West JL, Cancer Letters. 2004, 209,171-176.
13. Brabury J, Lancet Oncology, 2003;4:711.
14. Brongersma ML, Nature Materials. 2003;2:296-297.
15. Transportation Research Board Nanotechnology in concrete materials: A synopsis. Transportation research circular number E-C170; c2012.
16. Zhu R, Liu XN, Hu GK, Sun CT, Huang GL. Negative refraction of elastic waves at the deep-subwavelength in a single-phase met material. Nature Communications; c2014.
17. Ugwu OO, Arop JB, Nwoji CU, Osadebe N. Nanotechnology as a preventive engineering solution to highway infrastructure failures. J Constr Eng Manag; c2013 Aug. p. 987-993.
18. Pacheco-Torgal F, Jalali S. Nanotechnology advantages and drawbacks in the field of construction and building materials. Construction and Building Materials. 2011;25:582-590.
19. Gohardani O, Elola MC, Elizetxea C. Potential and prospective implementation of carbon nanotubes on next generation aircraft and space vehicles: a review of current and expected applications in aerospace sciences. Progress in Aerospace Sciences. 2014;70:42-68.
20. Malucelli G, Carosio F, Alongi J, Fina A, Frache A. Materials engineering for surface-confined flame retardancy. Mat SciEng R Rep. 2014;84:1-20.